

## Synthesis and Conducting Properties of a New Mixed-valence Cu(I)–Cu(II) 1-D Coordination Polymer Bridged by Morpholine Dithiocarbamate

Kyung Ho Kim,<sup>1,†</sup> Takashi Ueta,<sup>1</sup> Takashi Okubo,<sup>\*1</sup> Shinya Hayami,<sup>2</sup> Haruho Anma,<sup>1</sup> Kazuya Kato,<sup>2</sup> Tetsuya Shimizu,<sup>2</sup> Junji Fujimori,<sup>1</sup> Masahiko Maekawa,<sup>1</sup> and Takayoshi Kuroda-Sowa<sup>\*1</sup>

<sup>1</sup>School of Science and Engineering, Kinki University, 3-4-1 Kowakae, Higashi-Osaka, Osaka 577-8502

<sup>2</sup>Department of Chemistry, Faculty of Science, Kumamoto University, 39-1 Kurokami 2-chome, Kumamoto 860-8555

(Received June 16, 2011; CL-110506; E-mail: okubo.t@chem.kindai.ac.jp)

A novel mixed-valence Cu(I)–Cu(II) coordination polymer with an infinite one-dimensional (1-D) structure,  $[\text{Cu}^{\text{I}}_4\text{Cu}^{\text{II}}\text{I}_4(\text{Mor-dtc})_2(\text{CH}_3\text{CN})_2]_n$  (Mor-dtc<sup>-</sup>: morpholine dithiocarbamate), was prepared and structurally characterized by X-ray diffraction. This complex consists of a mononuclear copper(II) unit of  $[\text{Cu}^{\text{II}}(\text{Mor-dtc})_2]$  and a tetranuclear Cu(I) unit of  $[\text{Cu}_4\text{I}_4(\text{CH}_3\text{CN})_2]$ . It also shows semiconductive behaviors with a relatively small activation energy, which was revealed by impedance analysis.

Coordination polymers have attracted considerable interest as a new class of organic–inorganic hybrid materials.<sup>1,2</sup> This is due to their unique infinite structures and electronic states formed by the combination of metal ions with versatile coordination architectures and a variety of organic bridging ligands. Conducting coordination polymers<sup>2</sup> are of particular importance and interest for both fundamental knowledge and a variety of technological applications.

We investigated the conducting properties of mixed-valence Cu(I)–Cu(II) coordination polymers including dithiocarbamate derivatives.<sup>3</sup> A three-dimensional coordination polymer,  $[\text{Cu}^{\text{I}}_4\text{Cu}^{\text{II}}\text{Br}_4(\text{Pyr-dtc})_4] \cdot \text{CHCl}_3$  (Pyr-dtc<sup>-</sup>: pyrrolidine dithiocarbamate),<sup>3a</sup> showed a relatively high carrier mobility ( $\Sigma\mu = 0.4 \text{ cm}^2 \text{ V}^{-1} \text{ s}^{-1}$ ) comparable to that of organic semiconductors used for devices such as P3HT ( $0.1 \text{ cm}^2 \text{ V}^{-1} \text{ s}^{-1}$ ),<sup>4a</sup> PTV ( $0.22 \text{ cm}^2 \text{ V}^{-1} \text{ s}^{-1}$ ),<sup>4b</sup> PNDTBT-16 ( $0.54 \text{ cm}^2 \text{ V}^{-1} \text{ s}^{-1}$ ),<sup>4c</sup> and pentacene ( $1.5 \text{ cm}^2 \text{ V}^{-1} \text{ s}^{-1}$ ).<sup>4d</sup> Mixed-valence one-dimensional coordination polymers,  $[\text{Cu}^{\text{I}}_2\text{Cu}^{\text{II}}\text{X}_2(\text{Hm-dtc})_2(\text{CH}_3\text{CN})_2]_n$  (Hm-dtc<sup>-</sup>: hexamethylene dithiocarbamate; X = Br<sup>-</sup> or I<sup>-</sup>),<sup>3b</sup> were also effective sensitizing materials for dye-sensitized solar cells.<sup>3c</sup> In this paper, we report a new mixed-valence coordination polymer containing a dithiocarbamate ligand and I anions,  $[\text{Cu}^{\text{I}}_4\text{Cu}^{\text{II}}\text{I}_4(\text{Mor-dtc})_2(\text{CH}_3\text{CN})_2]_n$  (**1**) (Mor-dtc<sup>-</sup>: morpholine dithiocarbamate). In the synthesis, an iron ion of the starting material  $[\text{Fe}(\text{Mor-dtc})_3]$  was replaced by a copper ion of the CuI reactant to form a mixed-valence Cu(I)–Cu(II) infinite structure, which was confirmed by X-ray diffraction, X-ray photoelectron spectroscopy (XPS), and X-ray fluorescence analysis, as reported below. In order to study its conductive properties, an impedance measurement of this mixed-valence coordination polymer was carried out.

Complex **1** was synthesized by the reaction of a dichloromethane solution of  $[\text{Fe}(\text{Mor-dtc})_3]$  with an acetone/acetonitrile solution of CuI, where  $[\text{Fe}(\text{Mor-dtc})_3]$  was employed as a starting material instead of  $[\text{Cu}(\text{Mor-dtc})_2]$  because it was difficult to synthesize  $[\text{Cu}(\text{Mor-dtc})_2]$  due to the strong reducing property to the Cu(II) ion. The reaction mixture was filtered, and black, single, needle-shaped crystals suitable for X-ray diffrac-

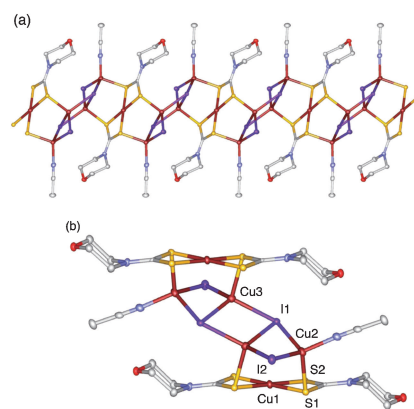


**Figure 1.** Crystal structures of the (a) infinite 1D chain and the (b) tetranuclear Cu(I) unit bridging mononuclear  $[\text{Cu}^{\text{II}}(\text{Mor-dtc})_2]$  units of complex **1**. Color code: Cu, red-brown; I, purple; S, yellow; C, white; N, blue; O, red. H atoms are omitted for clarity.

tion were obtained after a couple of days of slow diffusion into ether. The phase purity of the complex was identified by the comparison of the experimentally obtained X-ray powder diffraction (XRPD) patterns with ones simulated from its single-crystal structure (Figure S2<sup>11</sup>).

Figure 1a shows the 1-D infinite chain structure revealed by the single-crystal X-ray analysis of complex **1**.<sup>5</sup> Mononuclear copper units,  $[\text{Cu}(\text{Mor-dtc})_2]$ , are connected by a tetranuclear Cu(I) unit of  $[\text{Cu}_4\text{I}_4(\text{CH}_3\text{CN})_2]$  consisting of four tetrahedral Cu(I) ions, four bridging iodide ions, and two terminal acetonitrile moieties, as shown in Figure 1b. A symmetric unit includes two infinite chains with an isomorphous structure (Figure S1a<sup>11</sup>). The copper ions of the mononuclear units, Cu(1) and Cu(4), exhibit square-planar coordination geometries where in the Mor-dtc<sup>-</sup> ligands coordinate with the copper ion forming four-membered chelate rings. Usually, the oxidation states of Cu complexes with dithiocarbamate ligands can be determined through the Cu–S distances. In the mononuclear  $[\text{Cu}(\text{Mor-dtc})_2]$  unit of the coordination polymer **1**, the average Cu–S distance (2.3191(10) Å) is similar to reported average Cu(II)–S distances in Cu(II)–dithiocarbamate complexes such as  $[\text{Cu}^{\text{II}}(\text{Me}_2\text{dte})_2]$  (2.311 Å),  $[\text{Cu}^{\text{II}}(\text{Et}_2\text{dte})_2]$  (2.312 Å),  $[\text{Cu}^{\text{II}}(\text{MePh-dtc})_2]$  (2.287 Å),  $[\text{Cu}^{\text{II}}(n\text{-Bu}_2\text{dte})_2]$  (2.308 Å), and  $[\text{Cu}^{\text{II}}(\text{Bz}_2\text{dte})_2]$  (2.293 Å).<sup>6</sup> The Cu(2), Cu(3), Cu(5), and Cu(6) ions in the tetranuclear cluster units have distorted tetrahedral coordination geometries that are typical for Cu(I) ions. On the basis of its charge neutrality, it is concluded that complex **1** is in a mixed-valence state and that its chemical formula is  $[\text{Cu}^{\text{I}}_4\text{Cu}^{\text{II}}\text{I}_4(\text{Mor-dtc})_2(\text{CH}_3\text{CN})_2]_n$ .

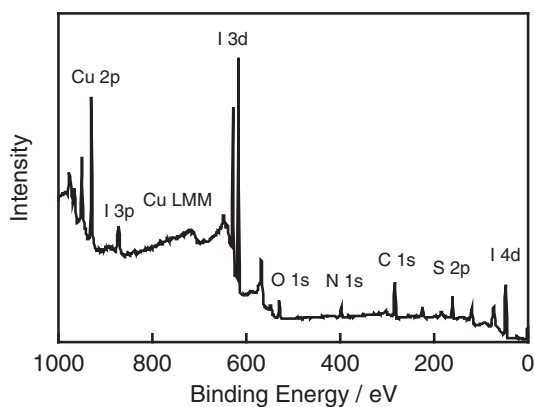


**Figure 2.** XPS survey spectrum of complex **1**.

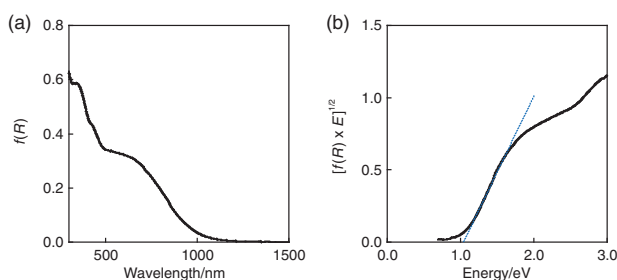


**Figure 3.** (a) Diffuse-reflection spectrum of complex **1** (0.01 mmol) mixed with MgO (80 mg). (b) Kubelka–Munk plot for the band gap evaluation of complex **1**.

In the synthesis of the mixed-valence coordination polymer, the iron ion in the starting material,  $[\text{Fe}(\text{Mor-dtc})_3]$ , was replaced by a copper ion, as determined by the X-ray structural analysis. The XPS analysis of the bulk sample confirms that the crystals do not contain any iron atoms. Figure 2 shows the XPS survey spectrum using  $\text{AlK}\alpha$  radiation. Peaks originating from Cu, C, N, O, S, and I atoms are clearly observed. However, no peaks around 710 eV corresponding to the  $\text{Fe } 2p_{3/2}$  atoms were evident. As shown in Figure S3a,<sup>11</sup> Cu LMM Auger signals were observed for complex **1** instead of Fe 2p signals. The X-ray fluorescence analysis also suggests that the amount of the contaminated iron ions in the polycrystalline sample are less than 1% of copper ions (Figure S4<sup>11</sup>).

Figure 3a shows the diffuse-reflection spectrum converted from diffuse reflectance ( $R$ ) using the Kubelka–Munk function:  $f(R) = (1 - R)^2/2R$ . Complex **1** exhibits broad absorptions in the UV to NIR region. The broad absorption at 595 nm may be attributed to the d–d transition of the Cu(II) ion. To determine the band gap ( $E_g$ ) of complex **1**, the Kubelka–Munk plot,<sup>7</sup>  $[f(R) \cdot E]^{1/2}$  versus  $E$  was employed (Figure 3b). The  $E_g$  corresponds to the intersection point between the baseline along the energy axis and a line extrapolated from the linear portion of the threshold. Thus,  $E_g$  of complex **1** was determined to be 1.1 eV.

Complex impedance spectroscopy (CIS) gives the electrical conductivity properties of materials as a function of temperature and frequency.<sup>8,9</sup> The impedance measurement was carried out using a pressed powder pellet sample sandwiched by brass electrodes (diameter, 13 mm); the thickness of the pellet sample

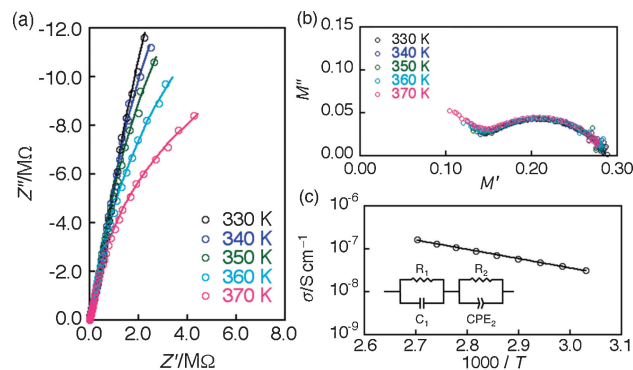


**Figure 4.** (a) Nyquist plots of complex **1** at various temperatures, (b) complex modulus plots, and (c) the temperature dependence of the bulk conductivity and equivalent circuit model.

of **1** was 0.131 mm. Figure 4a shows the complex impedance spectra over a wide range of frequencies within a temperature range of 330–370 K. In these plots, parts of the semicircular arcs are drawn and the diameters of the curvature decrease with increasing temperature, which means that this complex has typical semiconducting properties, i.e., a negative temperature coefficient of resistance (NTCR).

In general, the modulus spectrum shows a marked change in its shape with an increase in temperature indicating a probable change in the capacitance values of the materials as a function of temperature. Figure 4b shows the variation of the real ( $M'$ ) and imaginary ( $M''$ ) parts of the complex electric modulus over a range of temperatures. The complex modulus ( $M^*$ ) is given by the inverse of complex dielectric permittivity ( $\epsilon^*$ ).<sup>8,9</sup> The complex modulus diagram shows two well-defined regions: a semicircle in the high frequency region (right arc) due to the bulk (interior) and a semicircle in the low frequency region associated to the electrode interface. The diameter of the right arcs did not change with given temperatures, which implies a temperature-independent capacitance and indicates conductivity relaxation suggesting an impedance behavior in this system. The loss peak frequency ( $f$ ) of  $M''$  gives an estimation of the conduction relaxation time ( $\tau_\sigma$ ) according to the relaxation  $\omega_{\text{max}}\tau_\sigma = 1$ ,<sup>9</sup> where  $\omega_{\text{max}}$  is  $2\pi f$ . The value of the activation energy estimated from the slope of  $\ln \tau_\sigma$  against  $1/T$  curve is 0.44 eV.

To distinguish the parameters of bulk conductivity from the total AC conductivity of complex **1**, we used the equivalent circuit model of the ZView software,<sup>10</sup> which comprises series resistance ( $R_1$  and  $R_2$ ), capacitance ( $C_1$ ), and constant phase element (CPE<sub>2</sub>) as shown in Figure 4c. The intercepts of the semicircular arcs with the real axis ( $Z'$ ) in Figure 4a give an estimate of the bulk resistance ( $R_1$ ) and resistance ( $R_2$ ) of the electrode interface of complex **1**. This is because the Nyquist plot comprises a first semicircle at high frequency (bulk element) and a second semicircle at low frequency (electrode interface). The values of the bulk resistance of complex **1** were estimated from the complex impedance spectra as a function of temperature. Figure 4c shows the temperature dependence of the bulk conductivity of complex **1**. It is calculated using the relation  $\sigma = d/R_1S$ , where  $d$  (0.0131 cm) and  $S$  (1.33 cm<sup>2</sup>) are the

thickness and cross-sectional area of the pellet, respectively. It was observed that the bulk conductivity increases with an increase in temperature. The value of the bulk conductivity at room temperature (300 K), as estimated by the extrapolation of the straight line in Figure 4c, was found to be  $6.9 \times 10^{-9} \text{ S cm}^{-1}$ . The transport of charge carriers through the 1-D chain plays a major role in the electrical conductivity of complex **1**. The activation energy ( $E_a$ ) of bulk conductivity, which is calculated from the slope of the Arrhenius plots ( $\ln \sigma$  vs.  $1000/T$ ), is about 0.41 eV. This is in good agreement with the value calculated from the relaxation of the activation energy. It means that complex **1** is an intrinsic semiconductor.

Most coordination polymers are insulating, but conduction bands can be created with the proper choice of metal centers and bridging ligands. The electrical activation energy  $E_a$  of the coordination polymer **1** is smaller than those of 1-D coordination polymers,  $[\text{Cu}^1_2\text{Cu}^{\text{II}}\text{Br}_2(\text{Hm-dtc})_2(\text{CH}_3\text{CN})_2]_n$  ( $\sigma_{340\text{K}} = 1.1 \times 10^{-7} \text{ S cm}^{-1}$ ,  $E_a = 0.56 \text{ eV}$ ),  $[\text{Cu}^1_2\text{Cu}^{\text{II}}\text{I}_2(\text{Hm-dtc})_2(\text{CH}_3\text{CN})_2]_n$  ( $\sigma_{340\text{K}} = 2.5 \times 10^{-7} \text{ S cm}^{-1}$ ,  $E_a = 0.56 \text{ eV}$ ),<sup>3b</sup> and a 2-D coordination polymer  $[\text{Rh}(\text{pid})\text{Cl}]_n$  ( $\sigma_{\text{rt}} = 2 \times 10^{-12} \text{ S cm}^{-1}$ ,  $E_a = 0.45 \text{ eV}$ );<sup>2i</sup> and larger than those of 3-D coordination polymers,  $\{[\text{Cu}^1_4\text{Cu}^{\text{II}}_2\text{Br}_4(\text{Pyr-dtc})_4] \cdot \text{CHCl}_3\}_n$  ( $\sigma_{300\text{K}} = 5.2 \times 10^{-7} \text{ S cm}^{-1}$ ,  $E_a = 0.29 \text{ eV}$ )<sup>3a</sup> and  $\text{Cu}^1[\text{Cu}^{\text{III}}(\text{pds})_2]$  ( $\sigma_{300\text{K}} = 6 \times 10^{-4} \text{ S cm}^{-1}$ ,  $E_a = 0.19 \text{ eV}$ ).<sup>2c</sup>

In summary, we synthesized a new mixed-valence 1-D coordination polymer from  $[\text{Fe}(\text{Mor-dtc})_3]$ . This complex shows semiconductor behaviors with a relatively small activation energy. It also exhibits temperature-dependent relaxation phenomena.

This work was partly supported by PRESTO (JST), a Grant-in-Aid for Science Research from the Ministry of Education, Culture, Sports, Science and Technology of Japan, and “Development of Molecular Devices in Ferroelectric Metallomesogens” from New Energy and Industrial Technology Development Organization (NEDO).

## References and Notes

† Present address: Department of Materials Science, Faculty of Engineering, Kitami Institute of Technology, 165 Koen-cho, Kitami, Hokkaido 090-8507

1 O. M. Yaghi, M. O’Keeffe, N. W. Ockwig, H. K. Chae, M. Eddaoudi, J. Kim, *Nature* **2003**, *423*, 705; S. Kitagawa, R. Kitaura, S.-i. Noro, *Angew. Chem., Int. Ed.* **2004**, *43*, 2334; S.-i. Noro, *Phys. Chem. Chem. Phys.* **2010**, *12*, 2519; R.-Q. Zou, H. Sakurai, Q. Xu, *Angew. Chem., Int. Ed.* **2006**, *45*, 2542; S.-H. Cho, B. Ma, S. T. Nguyen, J. T. Hupp, T. E. Albrecht-Schmitt, *Chem. Commun.* **2006**, 2563; T. Uemura, R. Kitaura, Y. Ohta, M. Nagaoka, S. Kitagawa, *Angew. Chem., Int. Ed.* **2006**, *45*, 4112; D. Farrusseng, S. Aguado, C. Pinel, *Angew. Chem., Int. Ed.* **2009**, *48*, 7502; O. Kahn, *Molecular Magnetism*, VCH, New York, **1993**; S. Ferlay, T. Mallah, R. Ouahès, P. Veillet, M. Verdaguer, *Nature* **1995**, *378*, 701; O. Sato, T. Iyoda, A. Fujishima, K. Hashimoto, *Science* **1996**, *271*, 49; Q. Ye, Y.-M. Song, G.-X. Wang, K. Chen, D.-W. Fu, P. W. H. Chan, J.-S. Zhu, S. D. Huang, R.-G. Xiong, *J. Am. Chem. Soc.* **2006**, *128*, 6554; W. Zhang, R.-G. Xiong, S. D. Huang, *J. Am. Chem. Soc.* **2008**, *130*, 10468.

2 a) K. Otsubo, A. Kobayashi, H. Kitagawa, M. Hedo, Y.

Uwatoko, H. Sagayama, Y. Wakabayashi, H. Sawa, *J. Am. Chem. Soc.* **2006**, *128*, 8140. b) M. Mitsumi, T. Murase, H. Kishida, T. Yoshinari, Y. Ozawa, K. Toriumi, T. Sonoyama, H. Kitagawa, T. Mitani, *J. Am. Chem. Soc.* **2001**, *123*, 11179. c) H. Miyasaka, N. Motokawa, S. Matsunaga, M. Yamashita, K. Sugimoto, T. Mori, N. Toyota, K. R. Dunbar, *J. Am. Chem. Soc.* **2010**, *132*, 1532. d) M. Tadokoro, S. Yasuzuka, M. Nakamura, T. Shinoda, T. Tatenuma, M. Mitsumi, Y. Ozawa, K. Toriumi, H. Yoshino, D. Shiomi, K. Sato, T. Takui, T. Mori, K. Murata, *Angew. Chem., Int. Ed.* **2006**, *45*, 5144. e) S. Takaishi, M. Hosoda, T. Kajiwara, H. Miyasaka, M. Yamashita, Y. Nakanishi, Y. Kitagawa, K. Yamaguchi, A. Kobayashi, H. Kitagawa, *Inorg. Chem.* **2009**, *48*, 9048. f) S. Ichikawa, S. Kimura, K. Takahashi, H. Mori, G. Yoshida, Y. Manabe, M. Matsuda, H. Tajima, J.-i. Yamaura, *Inorg. Chem.* **2008**, *47*, 4140. g) P. Amo-Ochoa, O. Castillo, S. S. Alexandre, L. Welte, P. J. de Pablo, M. I. Rodríguez-Tapiador, J. Gómez-Herrero, F. Zamora, *Inorg. Chem.* **2009**, *48*, 7931. h) J. C. Zhong, Y. Misaki, M. Munakata, T. Kuroda-Sowa, M. Maekawa, Y. Suenaga, H. Konaka, *Inorg. Chem.* **2001**, *40*, 7096. i) C. G. Carson, R. A. Gerhardt, R. Tannenbaum, *J. Phys. Chem. B* **2007**, *111*, 14114.

3 a) T. Okubo, N. Tanaka, K. H. Kim, H. Anma, S. Seki, A. Saeki, M. Maekawa, T. Kuroda-Sowa, *Dalton Trans.* **2011**, *40*, 2218. b) T. Okubo, N. Tanaka, K. H. Kim, H. Yone, M. Maekawa, T. Kuroda-Sowa, *Inorg. Chem.* **2010**, *49*, 3700. c) K. H. Kim, T. Okubo, N. Tanaka, N. Mimura, M. Maekawa, T. Kuroda-Sowa, *Chem. Lett.* **2010**, *39*, 792.

4 a) H. Siringhaus, N. Tessler, R. H. Friend, *Science* **1998**, *280*, 1741. b) H. Fuchigami, A. Tsumura, H. Koezuka, *Appl. Phys. Lett.* **1993**, *63*, 1372. c) I. Osaka, T. Abe, S. Shinamura, E. Miyazaki, K. Takimiya, *J. Am. Chem. Soc.* **2010**, *132*, 5000. d) Y.-Y. Lin, D. J. Gundlach, S. F. Nelson, T. N. Jackson, *IEEE Electron Device Lett.* **1997**, *18*, 606.

5 Crystal data for  $[\text{Cu}^1_4\text{Cu}^{\text{II}}_4(\text{Mor-dtc})_2(\text{CH}_3\text{CN})_2]_n$ : fw 1231.94, triclinic,  $P1$ ,  $a = 7.9811(2) \text{ \AA}$ ,  $b = 12.1148(7) \text{ \AA}$ ,  $c = 15.8321(11) \text{ \AA}$ ,  $\alpha = 87.137(10)^\circ$ ,  $\beta = 85.415(8)^\circ$ ,  $\gamma = 75.549(7)^\circ$ ,  $V = 1476.9(2) \text{ \AA}^3$ ,  $Z = 2$ ,  $D_{\text{calcd}} = 2.770 \text{ g cm}^{-3}$ , 12488 reflections measured, 5191 independent.  $R_1 = 0.0192$  ( $I > 2.00\sigma(I)$ ),  $wR_2 = 0.0443$  (all data). CCDC: 826440.

6 F. Jian, Z. Wang, Z. Bai, X. You, H.-K. Fun, K. Chinnakali, I. A. Razak, *Polyhedron* **1999**, *18*, 3401; S. C. Ngo, K. K. Banger, M. J. DelaRosa, P. J. Toscano, J. T. Welch, *Polyhedron* **2003**, *22*, 1575.

7 P. Kubelka, F. Munk, *Zh. Tekh. Fiz.* **1931**, *12*, 593; M. H. Groothaert, P. J. Smeets, B. F. Sels, P. A. Jacobs, R. A. Schoonheydt, *J. Am. Chem. Soc.* **2005**, *127*, 1394.

8 B. Behera, P. Nayak, R. N. P. Choudhary, *Mater. Chem. Phys.* **2007**, *106*, 193; S.-P. Szu, C.-Y. Lin, *Mater. Chem. Phys.* **2003**, *82*, 295; K. P. Chandra, K. Prasad, R. N. Gupta, *Physica B (Amsterdam, Neth.)* **2007**, *388*, 118.

9 M. Nadeem, M. J. Akhtar, A. Y. Khan, *Solid State Commun.* **2005**, *134*, 431; M. Sural, A. Ghosh, *Solid State Ionics* **2000**, *130*, 259.

10 D. Johnson, *ZView: A Software Program for IES Analysis, Version 3.1*, Scribner Associates Inc., Southern Pines, NC, **2009**.

11 Supporting Information is available electronically on the CSJ-Journal Web site, <http://www.csj.jp/journals/chem-lett/index.html>.